

Effect of Strain Ranges and Phase Angles on the Thermomechanical Fatigue Properties of Thermal Barrier Coating System

Huang Feng¹, Nie Ming¹, Lin Jiedong¹, Hua Xu², Chen Guofeng², Zhou Zhongjiao³

¹ Electric Power Research Institute, Guangdong Power Grid Co. Ltd, Guangzhou 510080, China; ² Corporate Technology, Siemens, Shanghai 200082, China; ³ Division of Micro/Nano Manufacturing, State Key Laboratory of Tribology, Tsinghua University, Beijing 100084, China

Abstract: Thermal barrier coatings (TBCs) are the key material of components used in elevated temperature of gas turbines, and their mechanism of delamination and failure under service conditions has been the hot spot of research for a long time. The influences of strain ranges and phase angles on the thermomechanical fatigue (TMF) properties of samples with TBCs were investigated. It is shown that under the same phase angles, the TMF lifetime decreases with the increase of strain ranges. Under the same strain range, the in-phase tests have longer TMF lifetime than out-of-phase tests. In both samples, cracks are initiated in thermally grown oxide (TGO) layer, and then propagate along the bond coat/ceramic top coat, forming the delamination cracks. When the delamination cracks connect with the segmentation cracks initiated in ceramic coat, the TBCs spall. A TMF lifetime model concerning strain ranges and phase angles is established, and an exponential law exists between TMF lifetime and the maximum stress.

Key words: Ni-base superalloy; thermal barrier coatings; thermomechanical fatigue properties; lifetime model

Gas Turbine has been widely utilized in the industry, power generation and aviation fields recently^[1]. To achieve a higher working and energy efficiency of gas turbine, the inlet temperature elevates gradually from 900 °C to 1425 °C. This brings about many negative effects at high temperature, such as oxidation, and hot corrosion. Hence the protective thermal barrier coatings (TBCs) get applied by overlaying the superalloy substrate due to their heat-insulation, anti-corrosion performance^[2-4].

Generally, a TBC component is a multilayer system consisting of a ceramic top coat (TC), a metallic bond coat (BC) and a superalloy substrate^[5,6]. Usually, the TC is about 6~8 wt% Y₂O₃ stabilized ZrO₂ (YSZ) applied either by air plasma spraying (APS) or by electron-beam physical vapor deposition (EB-PVD). The purpose of the BC, typically a MCrAlY (M=Ni, Co, or NiCo), is dual. It improves the adherence of the TC to the substrate and acts as an oxidation barrier for the substrate. In addition, during the coating process and later in service at high temperatures, a

thermally grown oxide (TGO) layer, which mostly consists of stable α -Al₂O₃, develops between the BC and the TC^[7].

During service, the gas turbine blades endure high level dynamic mechanical stress as well as rapidly changing temperatures. The thermomechanical fatigue (TMF) is a major lifetime limiting factor, which causes the delamination of the ceramic TC from the BC and the loss of the TBCs^[8-11]. This accelerates localized oxidation or might even lead to local melting at high gas temperatures, thus promoting failure of the components. The complex process of TBC degradation^[12] is affected by: (1) growth of the TGO and thermal-expansion mismatch strains and stresses at the metal-ceramic interface; (2) temperature gradient across the TBCs and sintering processes in the TBCs, which affect stiffness, thermal conductivity and crack resistance; (3) diffusion of elements from the base material and BC to the interface; (4) cyclic plastic and time dependent deformation, as well as stress relaxation, etc.

The TMF life for TBC systems is influenced by many

Received date: December 11, 2016

Corresponding author: Zhou Zhongjiao, Ph. D., Division of Micro/Nano Manufacturing, State Key Laboratory of Tribology, Tsinghua University, Beijing 100084, P. R. China, E-mail: zhouzhongjiao2006@163.com

Copyright © 2017, Northwest Institute for Nonferrous Metal Research. Published by Elsevier BV. All rights reserved.

factors, such as sample sizes, strain ranges, phase angles, temperature ranges, heating and cooling rate. Among these factors, it was found that the relationship of the lifetime for TBC systems between in-phase (IP) TMF and out-of-phase (OP) TMF is variable. Wright^[13] found that the OP TMF lifetime of the TBC system was longer than the IP TMF one, whereas Baufeld's experiments^[14,15] revealed that the IP TMF lifetime was longer. In addition, though many works have been done about the influence of strain ranges, not a universally quantitative assessment of strain ranges was given. Therefore, a TMF lifetime model is desperately needed to understand the failure behavior of TBC systems under service conditions and to predict the lifetime of the components.

The main purpose of the present work was to investigate the influence of strain ranges and phase angles on TMF behavior of TBC systems and find out a universally quantitative TMF lifetime model of TBC systems considering the two factors.

1 Experiment

In the present study, the columnar crystal superalloy MGA1400 was chosen as the substrate material and was manufactured to TMF cylindrical specimens with a gauge diameter of 6 mm and a gauge length of 15 mm according to Fig.1. Then, all the substrates were grit blasted by alumina powder with 80 mesh grain size distribution. Afterwards, the substrate was deposited by High Velocity Oxygen Fuel (HVOF) with a CoNi32Cr32Al8Y0.5 alloy as the BC with the thickness between 80 μm and 100 μm . The 8 wt% yttria Y_2O_3 partially stabilized ZrO_2 (YSZ) ceramic TC was deposited by means of air plasma spraying (APS) with thickness between 300 μm and 320 μm , as shown in Fig.2.

The TMF tests were performed on an MTS810 closed-loop servo-hydraulic test machine with computer control. A radiation furnace powered by four cylindrical quartz lamps, each with a maximum power of 2.5 kW was used for heating. Cooling was mainly achieved by thermal conduction into the water cooling specimen grips and forced by blowing compressed air. Axial strain measurements were obtained using a self-supporting extensometer which has a gauge length of 16 mm and was supported with ceramic rods.

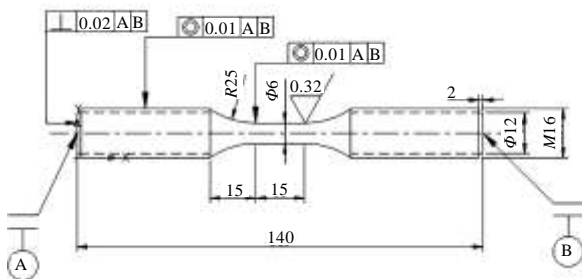


Fig.1 TMF specimen geometry

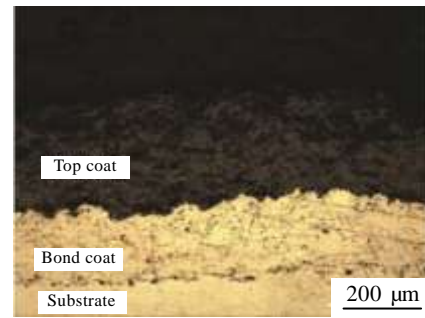


Fig.2 Microstructure of the as-deposited TBC

Temperature control was conducted with a thermocouple enclined in the middle of the gauge length. In order to reduce the amount of time that one single specimen remains in the TMF tests, the specimens were isothermally pre-oxidized at 1000 $^{\circ}\text{C}$ in air for 100 h prior to the TMF experiments. To closely represent turbine engine conditions, a dwelling time 5 min at the highest temperature was included in tests (Fig.3).

Two kinds of TMF loading were used: IP where the maximum mechanical strain coincides with the maximum temperature and OP where the maximum mechanical strain is attained at the minimum temperature. TMF tests were carried out in the temperature range of 200–900 $^{\circ}\text{C}$ with a cyclic period of 900 s under mechanical strain control. The mechanical strain ranges, $\Delta\epsilon_{\text{mech}} = \epsilon_{\text{max}} - \epsilon_{\text{min}}$, are -0.45% , -0.30% and 0.30% , as listed in Fig.3.

After the TMF tests, the specimens were embedded in an epoxy resin before cutting to reduce the possibility of damage, and then longitudinal and horizontal sections of the tested specimens were cut. Then these sections were metallographically prepared and observed by the optical microscopy (OM) and scanning electric microscopy (SEM).

2 Results

2.1 TMF lifetime

TBC spallation occurred after various numbers of cycles and the spallation geometries were observed in Fig.4. It was shown that phase angles and strain ranges have obvious influence on TMF lifetime (TBCs spallation), especially strain ranges. Under the same strain range 0.30%, the TBC coating got spalled after 69 cycles under IP tests (sample 3 in Fig.4) and a little shorter lifetime of 65 cycles under OP tests (sample 2 in Fig.4). With increasing compressive strain range to -0.45% , the coating OP life was shortened to only 5 cycles (sample 1 in Fig.4).

2.2 Cyclic stress-strain response

Fig.5 shows the comparison of hysteresis loops of 1st cycle and half life cycle under various TMF tests. It was shown that OP tests lead to severe inelastic deformation during the first cycle. The compressive stress increases up to 990 $^{\circ}\text{C}$ and thereafter it decreases despite the continuously

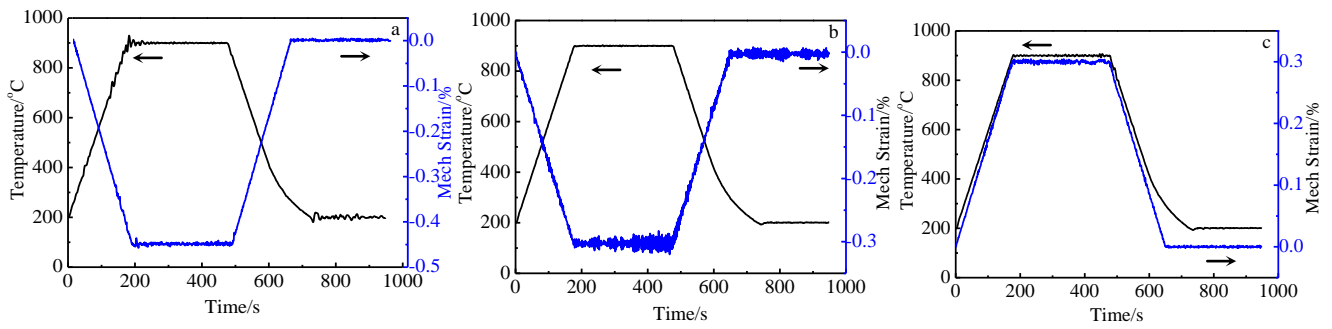


Fig.3 TMF cycles (200~900 °C) with pre-oxidation 100 h and a dwell time at high temperature applied to TBC: (a) $\Delta\varepsilon=-0.45\%$, OP, (b) $\Delta\varepsilon=-0.30\%$, OP, and (c) $\Delta\varepsilon=0.30\%$, IP



Fig.4 Spallation of TBC systems (1- $\Delta\varepsilon=-0.45\%$, OP; 2- $\Delta\varepsilon=-0.30\%$, OP; 3- $\Delta\varepsilon=0.30\%$, IP)

increasing compressive mechanical strain. Due to this inelastic deformation, the curves of the stress response are shifted upwards with increasing cycle numbers. With increasing strain range from -0.45% to -0.30% , the maximum tensile stresses decrease, e.g. the maximum tensile stress increases from 400 MPa for $\Delta\varepsilon=-0.45\%$ to 100 MPa for $\Delta\varepsilon=-0.30\%$. Compared to OP tests, IP test lead to less inelastic deformation during the first cycle. The curves of the stress response are shifted downwards with increasing cycle numbers.

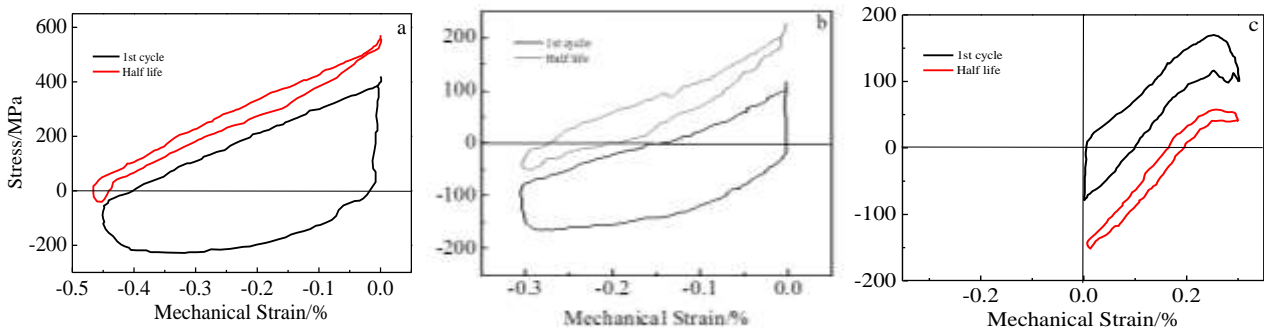


Fig.5 Hysteresis loops of 1st cycle and half life cycle for various TMF tests: (a) $\Delta\varepsilon=-0.45\%$, OP, (b) $\Delta\varepsilon=-0.30\%$, OP, and (c) $\Delta\varepsilon=0.30\%$, IP

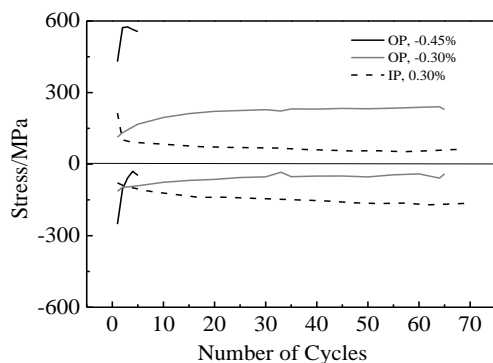


Fig.6 Cyclic stress response curves for varied TMF tests

The cyclic stress response behavior of various tests is shown in Fig.6, which displays the evolution of the maximum stress and the minimum stress with the number of cycles. In OP tests, the maximum tensile stress gradually increases and the maximum compressive stress decreases slightly with the increase of cycles. However, in IP tests, the tendencies of maximum tensile stress and the minimum compressive stress are just opposite.

2.3 TBC morphology after TMF tests

Typical cross-sections close to the spallation area is shown in Fig.7. Obvious delamination cracks (crack 1) along the BC/TC interface could be seen in Fig.7a. In zoomed view

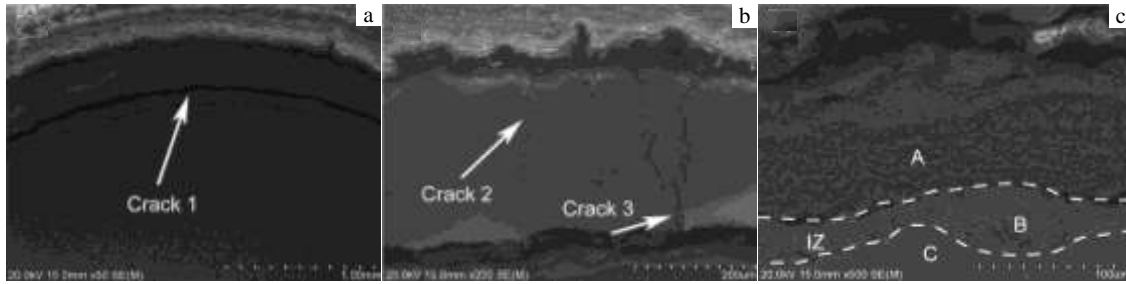


Fig.7 Cross-section morphologies of TMF samples with OP, $\Delta\epsilon=-0.45\%$

Table 1 EDS analysis for area A, B and C in Fig.7c (wt%)

Area	Ni	Co	Cr	Al	O
A	35.01	35.41	24.32	3.45	1.81
B	37.48	31.11	22.34	6.74	2.33
C	45.09	16.49	20.73	2.87	-

of TC (Fig.7b), some segmentation cracks initiate from the valley regions of TC surface (crack 2) and the BC/TC interface (crack 3) are present. A more detailed view of BC/substrate interface is shown in Fig.7c. Obviously, a thick interdiffusion zone (IZ) between BC and substrate is formed. The IZ has lost the columnar crystal orientation and the recrystallization could be clearly seen. EDS results (in Table 1) show that Co and Al diffuse from BC to the superalloy substrate, resulting in the diffusion front moving towards the substrate.

3 Discussion

3.1 Stress response of TMF tests

During OP-TMF tests, the maximum compressive mechanical loading at maximum temperature leads to severe inelastic compressive deformation during the first cycle, which results in a cyclic shift of the stress response into the tensile regime. Eventually, a critical tensile stress builds up at minimum temperature by the plastic ratcheting effect. Furthermore, relaxation of the stress occurs during dwelling at 900 °C^[16]. This reduction of the compressive stress (corresponding to compressive inelastic strain) results in the curves of the stress response shifting upwards with cycle numbers. However, in IP tests, the maximum tensile mechanical loading at maximum temperature leads to severe inelastic tensile deformation during the first cycle. The stress relaxation during dwelling at 900 °C makes the stress response curves shifting downwards with cycle numbers.

3.2 TMF lifetime model

It's well known that a TBC component is a multilayer system consisting of a ceramic TC, a BC, TGO and the superalloy substrate. According to Wright^[13] and Chen^[17], during TMF tests, besides the applied mechanical strain, thermal expansion mismatch strains exist due to the thermal

expansion and elastic module mismatch between TC, TGO, BC and Base metal. However, in their models, they ignored the complex microstructure of TBC systems and considered the whole TBC systems as one single layer. In addition, only thermal expansion coefficient mismatch was considered, while elastic module mismatch exists and also plays an important role on stress distribution of TBC systems.

Therefore, in our present work, various layers in TBC systems are considered, as well as thermal coefficient expansion and elastic module mismatch, as illustrated in Fig.8. Consequently, the total axial stress on the each layer of coating should be calculated as follows:

$$\Delta\sigma_{\text{total}} = \Delta\sigma_{\text{mech}} + \Delta\sigma_{\text{th}} = E\Delta\epsilon_{\text{mech}} + \Delta\sigma_{\text{th}} \quad (1)$$

The stress state of the coating is actually biaxial, namely, including the axial and circumferential stress. Generally, the axial stress is more related to the TMF lifetime of substrates, while the circumferential stress is suggested to be a dominating factor for the delamination and spallation of the coating^[13]. Delamination of the TBC layer occurs under the influence of tensile stresses acting perpendicular to BC/TC interface^[11]. In our present work, the tests are interrupted when TBC delamination and spallation occur, so more emphasis is put on the calculation of circumferential stress. Since the thermal mismatch strain acts in all directions equally and the transverse component of the applied mechanical stress is $-\nu E\Delta\epsilon_{\text{mech}}$ (ν is the Poisson's ratio), the circumferential stress can be calculated as:

$$\Delta\sigma_{\text{total}} = \Delta\sigma_{\text{mech}} + \Delta\sigma_{\text{th}} = -\nu E\Delta\epsilon_{\text{mech}} + \Delta\sigma_{\text{th}} \quad (2)$$

As for two different components i and j , with different coefficients of thermal expansion (α_i, α_j) and elastic module (E_i, E_j), the thermal mismatch stress is

$$\sigma_i = -\sigma_j = \frac{E_i E_j}{E_i + E_j} (\alpha_i - \alpha_j) \Delta T \quad (3)$$

Thus we can obtain the thermal mismatch stress of $\Delta\sigma_{\text{th}}^{\text{Base/BC}}$, $\Delta\sigma_{\text{th}}^{\text{BC/TGO}}$ and $\Delta\sigma_{\text{th}}^{\text{TGO/TC}}$ at the Base/BC, BC/TGO, TGO/TC interface, respectively. $\Delta T = T_{\text{max}} - T_{\text{middle}}$, where T_{middle} is the mid temperature of the tests. With those in mind, we can obtain the total circumferential stress of each layer as follows:

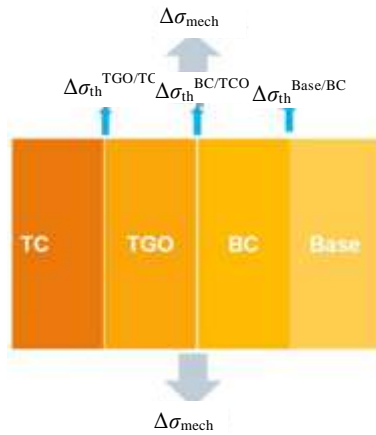


Fig.8 Sketch of stresses in the thermal barrier coating specimen

$$\text{BC layer, } \Delta\sigma_{\text{total}}^{\text{BC}} = -\nu E^{\text{BC}} \Delta\epsilon_{\text{mech}} + \Delta\sigma_{\text{th}}^{\text{Base/BC}} + \Delta\sigma_{\text{th}}^{\text{BC/TGO}} \quad (4)$$

$$\text{TGO layer, } \Delta\sigma_{\text{total}}^{\text{TGO}} = -\nu E^{\text{TGO}} \Delta\epsilon_{\text{mech}} + \Delta\sigma_{\text{th}}^{\text{BC/TGO}} + \Delta\sigma_{\text{th}}^{\text{TC/TGO}} \quad (5)$$

$$\text{TC layer, } \Delta\sigma_{\text{total}}^{\text{TC}} = -\nu E^{\text{TC}} \Delta\epsilon_{\text{mech}} - \Delta\sigma_{\text{th}}^{\text{TC/TGO}} \quad (6)$$

For IP or OP cycling, during heating stage, due to the fact that $\alpha_{\text{Base}} > \alpha_{\text{BC}} > \alpha_{\text{TC}} > \alpha_{\text{TGO}}$, tensile thermal expansion mismatch stress is produced on the Base and compressive stress on BC layer at the Base/BC interface. Similarly, tensile thermal expansion mismatch stress is produced on the BC layer and compressive stress on TGO layer at the BC/TGO interface, compressive stress on TGO layer and tensile stress on TC layer at the TGO/TC interface. With parameters such as elastic modulus, coefficient of thermal expansion and Poisson's ratio in Table 2^[18], the stress distribution of BC, TGO and TC layer can be calculated, as shown in Table 3.

In the present work, nonsymmetrical strain with $R=\infty$ is applied in TMF cycles and TBC spallation occurs both at the highest temperature corresponding to the largest mechanical strain (the largest tensile mechanical strain for IP and the largest compressive mechanical strain for OP). As for IP tests, the maximum stress in BC may lead to the crack initiation in BC/TGO interface and later TBC spallation. However, for OP tests, cracks may initiate at the TGO layer due to the maximum stress in TGO and propagate at the TGO/TC or TGO/BC interface, resulting in the delamination cracks in these interfaces.

Plotting the curve of TMF lifetime N_f vs the maximum stress σ_{max} (the maximum stress of TBC system) in Fig.9, it can be seen that an exponential law exists between N_f and σ_{max} , in the form of $N_f = a \cdot \exp(\sigma_{\text{max}}) + b$, which is similar to Wright's^[13] results, that is, an exponential law

Table 2 Parameters of TBC systems at 900 °C^[18]

Parameter	Base	BC (NiCoCrAlY)	TGO (Al ₂ O ₃)	TC (YSZ)
$\alpha / \times 10^{-6} \text{ K}^{-1}$	17.2	16.7	9.2	11.25
E/GPa	139	132	340	30
ν	0.34	0.33	0.24	0.11

Table 3 Stress distribution of TBC systems at 900 °C (MPa)

Layer	IP, 0.30%	OP, -0.30%	OP, -0.45%
BC	-356.58	-95.22	-206.30
TGO	24.1	513.7	636.1
TC	-29.2	-9.4	-4.45

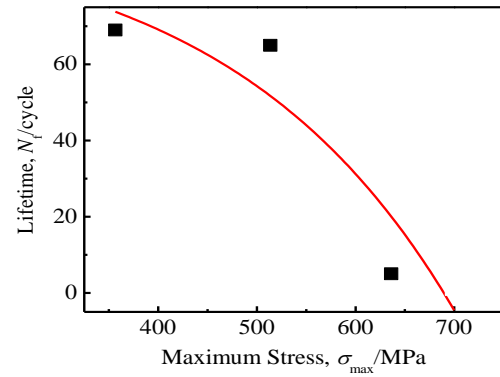


Fig.9 Dependence of TMF lifetime N_f on the maximum stress σ_{max}

exists between N_f and ϵ_{max} . With that, the TMF lifetime can be predicted by calculating the maximum stress in TBC systems, which is significantly meaningful to understand the failure behavior of TBC systems under service conditions and to predict the lifetime of the components.

4 Conclusions

1) Under the same phase angles, the TMF lifetime decreases with the increase of strain ranges. Under the same strain range, the IP tests have longer TMF lifetime than OP tests.

2) In both samples, cracks are initiated in TGO, then propagate along the bond coat/ceramic top coat, forming the delamination cracks. When the delamination cracks connect with the segmentation cracks in ceramic coat, the TBCs spall.

3) The dependence of TBC spallation lifetime on the maximum stress appears to fit reasonably well an exponential law.

Acknowledgement: Present work was supported by Guangdong Power Grid Co. Ltd, Electric Power Research and Corporate Technology, Siemens. The authors are grateful for these supports.

References

- 1 Guo Hongbo, Gong Shengkai, Xu Huibin. *Materials China* [J], 2009, 28(S2): 18 (in Chinese)
- 2 Miller R A. *Surface & Coatings Technology*[J], 1987, 30(1): 1
- 3 Miller R A. *Journal of Thermal Spray Technology*[J], 1997, 6: 35
- 4 Zhang Xiaofeng, Zhou Kesong, Chen Huantao et al. *Rare Metal Materials and Engineering*[J], 2015, 44(6): 1301
- 5 Clarke D R, Phillpot S R. *Materials Today*[J], 2005, 8(6): 22
- 6 Brindley W J, Miller R A. *Advanced Materials & Processes* [J], 1989, 136: 29
- 7 Lan Hao, Yang Zhigang, Zhang Yuduo et al. *Rare Metal Materials and Engineering*[J], 2012, 41(2): 194
- 8 Kraft S, Zauter R, Mughrabi H. *Fatigue & Fracture of Engineering Materials & Structures*[J], 1993, 16(2): 237
- 9 Bartsch M, Marci G, Mull K et al. *Advanced Engineering Materials*[J], 1999, 1(2): 127
- 10 Pahlavanyali S, Rayment A, Roebuck B et al. *International Journal of Fatigue*[J], 2008, 30(2): 397
- 11 Tzimas E, Müllejans H, Peteves S D et al. *Acta Materialia* [J], 2000, 48(18-19): 4699
- 12 Trunova O. *Thesis for Doctorate*[D]. Aachen: Publikationsserver der RWTH Aachen University, 2006
- 13 Wright P K. *Materials Science and Engineering A*[J], 1998, 245(2): 191
- 14 Baufeld B, Tzimas E, Hühner P et al. *Scripta Materialia*[J], 2001, 45(7): 859
- 15 Baufeld B, Tzimas E, Müllejans H et al. *Materials Science and Engineering A*[J], 2001, 315(1-2): 231
- 16 Aleksanoglu H, Scholz A, Oechsner M et al. *International Journal of Fatigue*[J], 2013, 53: 40
- 17 Chen Z B, Wang Z G, Zhu S J. *Materials Science and Engineering A*[J], 2011, 528(29-30): 8396
- 18 Zhou C G, Wang N, Xu H B. *Materials Science and Engineering A*[J], 2007, 452-453: 569

应变幅和相角度对热障涂层材料系统热机械疲劳性能的影响

黄 丰¹, 聂 铭¹, 林介东¹, 华 旭², 陈国锋², 周忠娇³

(1. 广东电网有限责任公司 电力科学研究院, 广东 广州 510080)

(2. 西门子中国研究院, 上海 200082)

(3. 清华大学 摩擦学国家重点实验室微纳制造分室, 北京 100084)

摘 要: 热障涂层作为燃气轮机高温部件的关键材料, 其服役过程中的脱落与失效机理一直是研究的热点问题。研究了应变幅和相角度对含热障涂层的镍基高温合金热机械疲劳性能的影响。研究表明, 在相同相角度下, 热机械疲劳寿命随应变幅的增大而降低。固定应变幅, 同相位下样品的热机械疲劳寿命要高于反相位样品。所有样品中, 裂纹萌生于热生长氧化物层, 在粘结层与陶瓷层界面扩展形成分层裂纹, 分层裂纹与陶瓷层内贯穿裂纹连接起来导致大面积的陶瓷层剥落, 从而导致TBC层失效。另外, 分析了热障涂层中的应力分布, 初步建立了含热障涂层的镍基高温合金热机械疲劳寿命模型, 发现含热障涂层的镍基高温合金热机械疲劳寿命与涂层中的最大应力呈指数关系。

关键词: 镍基高温合金; 热障涂层; 热机械疲劳性能; 寿命模型

作者简介: 黄 丰, 男, 1982 年生, 博士, 高级工程师, 广东电网有限责任公司电力科学研究院, 广东 广州 510080, E-mail: huanfen777@126.com